

Swinburne Research Bank

<http://researchbank.swinburne.edu.au>



Toscano, M., et al. (1999). Millisecond pulsar velocities

Originally published in *Monthly Notices of the Royal Astronomical Society*, 307(4), 925–933.

Available from: <http://dx.doi.org/10.1046/j.1365-8711.1999.02685.x>

Copyright © 1999 Royal Astronomical Society.

This is the author's version of the work, posted here with the permission of the publisher for your personal use. No further distribution is permitted. You may also be able to access the published version from your library. The definitive version is available at www.interscience.wiley.com.

Millisecond Pulsar Velocities

M. Toscano^{1,2}, J. S. Sandhu³, M. Bailes², R. N. Manchester^{4,1}, M. C. Britton²,
S. R. Kulkarni³, S. B. Anderson³, B. W. Stappers^{5*}

¹*Physics Department, University of Melbourne, Parkville, Vic 3052, Australia.*

²*Astrophysics and Supercomputing, Mail No. 31, Swinburne University of Technology, PO Box 218, Hawthorn, Vic 3122, Australia.*

³*Department of Astronomy, Caltech, Pasadena CA 91125.*

⁴*Australia Telescope National Facility, CSIRO, PO Box 76, Epping, NSW 2121, Australia.*

⁵*Mount Stromlo and Siding Spring Observatories, ANU, Private Bag, Weston Creek, ACT 2611, Australia.*

1 February 2008

ABSTRACT

We present improved timing parameters for 13 millisecond pulsars (MSPs) including 9 new proper motion measurements. These new proper motions bring to 23 the number of MSPs with measured transverse velocities. In light of these new results we present and compare the kinematic properties of MSPs with those of ordinary pulsars. The mean transverse velocity of MSPs was found to be $85 \pm 13 \text{ km s}^{-1}$; a value consistent with most models for the origin and evolution of MSPs and approximately a factor of four lower than that of ordinary pulsars. We also find that, in contrast to young ordinary pulsars, the vast majority of which are moving away from the Galactic plane, almost half of the MSPs are moving towards the plane. This near isotropy would be expected of a population that has reached dynamic equilibrium. Accurate measurements of MSP velocities have allowed us to correct their measured spin-down rates for Doppler acceleration effects, and thereby derive their intrinsic magnetic field strengths and characteristic ages. We find that close to half of our sample of MSPs have a characteristic age comparable to or greater than the age of the Galaxy.

Key words: pulsars: general – stars: kinematics

1 INTRODUCTION

The discovery of the first millisecond pulsar (MSP) by Backer et al. (1982) heralded the study of a distinct subclass of the pulsar population. The sixty or so MSPs discovered since then distinguish themselves from the ‘ordinary’ pulsar population not only by their shorter rotation periods but also by their greatly reduced spin-down rates, which imply much weaker magnetic fields and characteristic ages comparable to that of the Galactic disc. These properties, as well as the high incidence of MSPs in binary systems, suggest that MSPs and ordinary pulsars possess different evolutionary histories (Alpar et al. 1982; Radhakrishnan & Srinivasan 1981; Chanmugam & Brecher 1987; Bhattacharya & van den Heuvel 1991, and references therein).

MSPs are the paragon of rotational stability and allow us to develop timing models that can be used to predict the times of arrival (TOAs) of their radio pulses, in most cases with an uncertainty of the order of a few microseconds or

less. The millisecond periods that give MSPs their names greatly facilitate the process of pulsar timing and permit very precise astrophysical measurements to be made (Kaspi, Taylor, & Ryba 1994). Unlike ordinary pulsars which often show the deleterious effects of ‘timing noise’ over long periods of time, the level of such noise in MSPs does not prohibit the measurement of interesting physical parameters such as proper motion.

Proper motions of radio pulsars have been measured in a variety of ways. The original method employed conventional optical techniques to measure the proper motion of the Crab pulsar (Trimble 1971). However, this technique has only limited use since <1 per cent of pulsars are visible at optical wavelengths (Wyckoff & Murray 1977; Bignami & Caraveo 1988). The majority of pulsar proper motions have been measured using radio interferometric techniques (Lyne, Anderson, & Salter 1982; Bailes et al. 1990; Fomalont et al. 1992; Harrison, Lyne, & Anderson 1993; Fomalont et al. 1997). A radio-linked interferometer is used to measure the separation of the pulsar and an extragalactic reference source in terms of interferometric phase. Changes in this separation at different epochs yield the pulsar’s proper motion. A method used to determine pulsar speeds utilises

* Present Address: Astronomical Institute ‘Anton Pannekoek’, University of Amsterdam, Kruislaan 403, NL-1098SJ Amsterdam, The Netherlands.

measured changes in the pulsar’s interstellar scintillation (ISS) pattern. These changes are interpreted as the result of the pulsar’s motion relative to an hypothetical scattering screen midway between the observer and the pulsar (Cordes 1986). Proper motion measurements of pulsars based on arrival times were first made by Manchester, Taylor and Van (1974) and have been made for a number of pulsars since (Helfand, Taylor, & Manchester 1977; Rawley, Taylor, & Davis 1988; Bell et al. 1995). This technique is most applicable to pulsars with very low levels of timing noise since random timing irregularities can exhibit quasi-annual variations that may be misinterpreted as a positional offset or the pulsar’s motion. The exceptional timing stability of MSPs over periods of years makes them ideal candidates for proper motion studies. To date, proper motions have been measured for 14 MSPs using arrival-time methods: PSRs J0437–4715 (Sandhu et al. 1997); J0711–6830, J1024–0719, J1744–1134, and J2124–3358 (Bailes et al. 1997); B1257+12 (Wolszczan 1994); J1713+0747 (Camilo, Foster, & Wolszczan 1994); B1855+09 and B1937+21 (Kaspi, Taylor, & Ryba 1994); B1957+20 (Arzoumanian, Fruchter, & Taylor 1994); J2019+2425 and J2322+2057 (Nice & Taylor 1995); J2051–0827 (Stappers et al. 1998) and J2317+1439 (Camilo, Nice, & Taylor 1996). Thirteen MSPs have measured scintillation speeds: PSRs J0437–4715, J0711–6830, J1455–3330, J1603–7202, J1713+0747, J1730–2304, J1744–1134, J1911–1114, J2051–0827, J2124–3358, J2129–5718, J2145–0750 and J2317+1439 (Johnston, Nicastro, & Koribalski 1998).

Pulsars are, as a class, high-velocity objects. Lyne and Lorimer (1994) have suggested that pulsars are born with a mean velocity of $\sim 450 \text{ km s}^{-1}$. Although Hansen & Phinney (1997) have derived a lower mean velocity of $\sim 250 - 300 \text{ km s}^{-1}$, it is clear that pulsar velocities are, on average, about a factor of ten higher than those of their progenitor O and B stars. Two theories have been put forward to explain these high space velocities: (i) the progenitor (close) binary is disrupted because more than half the system mass is lost during the supernova (SN) explosion (Blaauw 1961; Gott, Gunn, & Ostriker 1970), and (ii) the pulsar receives a natal ‘kick’ resulting from the asymmetry of the SN event (Shklovskii 1970). The most likely explanation may well be a combination of both.

MSPs on the other hand have relatively low speeds compared with the general pulsar population. The known MSP proper motions imply a mean transverse velocity of $\sim 100 \text{ km s}^{-1}$. Although much work has been done to model the kinematics of ordinary pulsars, the lack of measured MSP proper motions has made constraining MSP velocity models difficult. Recently Tauris & Bailes (1996) made Monte Carlo simulations of a large ensemble of binary systems using a number of different evolutionary scenarios. The velocity distributions they derived had means of $\sim 110 \text{ km s}^{-1}$ assuming symmetric SNe explosions and $\sim 160 \text{ km s}^{-1}$ with the inclusion of random asymmetric kicks. Their models are consistent with observed transverse velocities. They also predict an anti-correlation between orbital period and recoil velocity (although this becomes weaker with the introduction of random kicks). Cordes & Chernoff (1997) have used a parametric likelihood analysis technique to model MSP dynamics. The MSPs they evolved were initially given velocities with an isotropic angular distribution and magnitudes

drawn from a Maxwellian distribution. This distribution of speeds had a dispersion of σ_V . Their analysis yielded as most likely $\sigma_V = 52^{+17}_{-11} \text{ km s}^{-1}$, a three-dimensional velocity dispersion of $\sim 84 \text{ km s}^{-1}$ and observed transverse speeds $< 200 \text{ km s}^{-1}$.

For nearby MSPs, there is another motivation for determining pulsar velocities. The transverse motion of nearby MSPs results in an apparent acceleration that makes a significant contribution to their measured spin-down rates (Shklovskii 1970). Knowing the transverse velocity and distances makes it possible to correct for this effect, extract the intrinsic spin-down rate, and thus calculate improved derived magnetic field strengths and characteristic ages. Corrected spin-down rates ensure that pulsars find their proper place in the $P-\dot{P}$ diagram from which physical conclusions may be drawn.

In §2 of this paper we describe our data collection and analysis methodology. In §3 we present improved timing parameters for 13 MSPs including nine new arrival-time proper motion measurements. The measurement of these new proper motions brings the number of MSPs with known transverse velocities to 23. In light of this, the aim of this paper is to bring together these results and investigate the kinematic properties that MSPs share as a class. To this end, in §4 we examine the velocity distribution of MSPs in the context of their origin and evolution. In particular we compare and contrast the velocities and dynamics of MSPs with those of ordinary pulsars. In §4 we also make use of these velocity measurements to derive intrinsic spin-down rates, magnetic field strengths and characteristic ages. §5 summarises our major findings.

2 OBSERVATIONS AND ANALYSIS

We used the Parkes 64-m radio telescope to make regular observations of the 17 MSPs discovered in the Parkes 70-cm survey (Manchester et al. 1996; Lyne et al. 1998) as well as a number of previously known MSPs visible from Parkes. The data presented in this paper has been collected since the end of 1994 using the Caltech correlator (Navarro 1994). Over this period, at low frequencies we used a dual linear polarisation system centred at 0.66 GHz with a system noise of 90 Jy. Initially, at high frequencies, we used a 1.4 GHz dual circular polarisation receiver with a system noise of 40 Jy. Since 1997 April, the centre receiver of the Parkes Multi-beam receiver system (dual linear polarisation and 26 Jy system noise) was used in its place. At 0.66 GHz we recorded a single 32 MHz band with 256 lags per polarisation. At 1.4 GHz, prior to 1995 July, a single intermediate-frequency (IF) band was recorded with 128 MHz of bandwidth and 256 lags per polarisation. This system was superseded by a dual-IF subsystem (Sandhu 1999) that made it possible to record two 128 MHz IFs with 128 lags per polarisation, centred on 1.4 and 1.66 GHz respectively.

The correlator is flexible enough to permit narrow-band observations with bandwidths of 64, 32, 16, 8 or 4 MHz using all the available lags. Diffractive interstellar scintillation results in a modulation of pulse intensity as a function of time and frequency, the time-scale and bandwidth of which increase with increasing frequency. For some MSPs, particularly at 0.66 GHz, a few scintles may be present across the

Table 1. Timing parameters for 13 MSPs

Pulsar	PSR J0613–0200	PSR J1045–4509	PSR J1455–3330	PSR J1603–7202
R. A. (J2000)	06 ^h 13 ^m 43 ^s .97336(2)	10 ^h 45 ^m 50 ^s .1927(1)	14 ^h 55 ^m 47 ^s .9618(3)	16 ^h 03 ^m 35 ^s .68523(5)
Decl. (J2000)	−02°00′47″.0970(7)	−45°09′54″.195(1)	−33°30′46″.350(7)	−72°02′32″.6517(5)
PM in R. A. (mas y ^{−1})	2.0(4)	−5(2)	5(6)	−3.5(3)
PM in Decl. (mas y ^{−1})	−7(1)	6(1)	24(12)	−7.8(5)
Galactic longitude	210°41	280°85	330°72	316°63
Galactic latitude	−9°30	12°25	22°56	−14°50
Period (ms)	3.06184403674401(5)	7.4742241060982(5)	7.987204795504(3)	14.8419520154668(2)
Period derivative (×10 ^{−20})	0.9572(5)	1.766(3)	2.42(1)	1.564(2)
Epoch (MJD)	50315.0	50277.0	50239.0	50427.0
Dispersion Measure (cm ^{−3} pc)	38.7792(1)	58.147(5)	13.578(7)	38.0501(1)
Orbital Period (days)	1.1985125566(4)	4.083529200(6)	76.1745675(6)	6.308629570(2)
a sin <i>i</i> (light-s)	1.0914441(5)	3.015134(2)	32.362233(5)	6.8806582(5)
Eccentricity	0.0000038(10)	0.0000197(13)	0.0001697(3)	0.0000092(1)
Epoch of periastron (MJD)	50315.38339(5000)	50276.26230(6000)	50275.16814(2000)	50426.11693(2000)
Longitude of periastron (deg)	34(14)	243(5)	223.78(9)	170.3(9)
Timing data span (MJD)	49700–50931	49623–50931	49700–50779	49922–50933
RMS timing residual (μs)	3.5	16.2	1.4	1.5
Number of timing points	122	141	25	144

observing bandwidth. In these cases it is feasible to centre an appropriately-sized narrow recording band over the scintillation maximum. The increased frequency resolution reduces dispersion smearing, and since most of the pulsar’s flux density is concentrated in the scintles, there is a significant gain in signal to noise ratio.

The baseband data were 2-bit digitised and the auto-correlation functions (ACFs) computed by the correlator were folded at the topocentric pulse period to form 90-s sub-integrations with 1024 bins per lag. The ACFs were corrected for the non-linear effects of the digitisation process and Fourier transformed to produce power spectra for each sub-integration. Narrow-band interference was rejected prior to dedispersion, the data were compressed to 32, 16 or 8 frequency channels and saved to disk. A typical observation consisted of a contiguous set of sixteen 90-s sub-integrations. Time synchronisation was provided by starting the first sub-integration coincident with the 10 s pulse from the observatory’s time system traceable to the NASA DSN at Tidbinbilla using a microwave link, and from there to UTC(NIST) via common-view Global Positioning System observations.

After summing the sub-integrations and frequency channels within each observation, the highest signal to noise ratio (SNR) profiles were added to form standard profiles for each observing frequency and pulsar. The standard profiles at each frequency were cross-correlated to determine their relative phase offset and phase-shifted to match. Pulse TOAs were determined by cross-correlating the 24-min integrated profiles with the corresponding standard profile. Arrival-time data were fitted to a pulse timing model using the TEMPO program (Taylor & Weisberg 1989). We used the DE200 ephemeris of the Jet Propulsion Laboratory (Standish 1982) to transform the TOAs to the solar system barycenter and the Blandford & Teukolsky (1976) model for timing pulsars in binary systems.

3 RESULTS

Of the 17 MSPs discovered in the Parkes 70-cm survey, we have eight binary and five isolated MSPs that show considerable improvement in timing accuracy compared with results published in their respective discovery papers (Bailes et al. 1994; Lorimer et al. 1995; Lorimer et al. 1996; Bailes et al. 1997). The timing parameters resulting from the best fits to the TOAs are shown in Table 1 where figures in parentheses represent 1σ uncertainties in the last significant digits quoted. Table 1 shows we now have finite values for the eccentricities of four MSPs where only upper bounds existed previously. Finite values for the spin-down rate of two MSPs have also replaced previous bounds. Proper motions are listed in Table 2. The nine pulsars for which we have new arrival-time proper motion measures are as follows; PSRs J0613–0200, J1045–4509, J1643–1224, J1455–3330, J1603–7202, J1730–2304, J1911–1114, J2129–5721 and J2145–0750. All but the first three MSPs have had their speeds determined in the scintillation study by Johnston et al. (1998) .

Our timing analysis of PSR J1744–1134 has yielded a measure of its parallax. The parallax of $\pi=2.7\pm 0.4$ mas corresponds to a distance of 370_{-47}^{+65} pc (Toscano et al. in preparation), significantly greater than the catalogued distance of 166 pc (Taylor, Manchester, & Lyne 1993). We have used this parallax-derived distance in our calculations.

The proximity of PSR J1730–2304 to the ecliptic makes measurement of its proper motion in declination difficult. Fitting for proper motion in ecliptic coordinates did not significantly improve the proper motion parameters. We have, however, used its motion in ecliptic longitude as a lower bound to its total proper motion.

The average time spanned by our data was ∼1130 days with an average of ninety 24 min observations per pulsar. Table 1 shows that the typical post-fit rms was under 2 μs. The majority of the fits returned values of χ^2/ν (where ν is the number of degrees of freedom) of between 1.3 and

Table 1. – continued

Pulsar	PSR J1643–1224	PSR J1911–1114	PSR J2129–5721	PSR J2145–0750
R. A. (J2000)	16 ^h 43 ^m 38 ^s .15583(4)	19 ^h 11 ^m 49 ^s .2927(2)	21 ^h 29 ^m 22 ^s .7539(3)	21 ^h 45 ^m 50 ^s .46813(4)
Decl. (J2000)	−12°24′58″.720(4)	−11°14′22″.33(2)	−57°21′14″.093(2)	−07°50′18″.361(2)
PM in R. A. (mas y ^{−1})	3(1)	−6(4)	7(2)	−9.1(7)
PM in Decl. (mas y ^{−1})	−8(5)	−23(13)	−4(3)	−15(2)
Galactic longitude	5°67	25°14	338°01	47°78
Galactic latitude	21°22	−9°58	−43°57	−42°08
Period (ms)	4.6216414465636(1)	3.6257455713977(5)	3.7263484187800(5)	16.0524236584091(2)
Period derivative (×10 ^{−20})	1.849(1)	1.416(8)	2.074(4)	2.986(1)
Epoch (MJD)	50288.0	50458.0	50444.0	50317.0
Dispersion Measure (cm ^{−3} pc)	62.4121(2)	30.9750(9)	31.855(4)	9.0006(1)
Orbital Period (days)	147.0173943(7)	2.71655761(1)	6.62549308(5)	6.838902510(1)
a sin <i>i</i> (light-s)	25.072613(1)	1.762875(5)	3.500559(3)	10.1641055(5)
Eccentricity	0.0005058(1)	0.0000188(55)	0.0000068(22)	0.0000193(1)
Epoch of periastron (MJD)	50313.03963(1000)	50455.59359(20000)	50442.60321(20000)	50313.71221(1000)
Longitude of periastron (deg)	321.810(9)	178(22)	178(12)	200.8(3)
Timing data span (MJD)	49645–50932	49982–50933	49983–50931	49703–50933
RMS timing residual (μs)	5.5	1.4	1.2	1.4
Number of timing points	126	35	66	80

2.9. To compensate for systematic effects we multiplied the TOA uncertainties by a factor of between 1.1 and 2.7 chosen such that χ^2/ν was unity. The trend in the TOAs for a small number of MSPs in our sample show low levels of unmodelled behaviour. The origin of these effects is most likely a combination of low signal to noise integrated profiles and the effects of radio frequency interference (RFI). At higher frequencies our data do not show the same extent of RFI contamination and therefore are a better measure of the intrinsic timing accuracy.

4 DISCUSSION

4.1 Pulsar velocities

4.1.1 Pulsar velocity distributions

The numerical modelling work of Tauris & Bailes (1996) and Cordes & Chernoff (1997) and the standard models for the formation of recycled pulsars (Bhattacharya & van den Heuvel 1991, and references therein) all suggest MSPs have velocities much lower than their long-period counterparts. These lower velocities are qualitatively understood in terms of the asymmetry of the SN explosion and the fraction of mass suddenly ejected from the system during this event. These elements depend upon the characteristics of the system prior to the SN which, in turn depend upon a number of factors including; the rate and duration of mass loss and/or transfer, the nature of the common-envelope phase of binary evolution, and the peculiar evolution of each star. The distinction between the velocities of ordinary pulsars and MSPs is evident from the histograms of pulsar velocities in Fig. 1. A Kolmogorov–Smirnov test shows that the probability that the respective velocities were drawn from the same distribution is $<10^{-5}$. Most of the ordinary pulsars have velocities up to 500 km s^{−1} with a small number of pulsars with velocities as high as ~ 1000 km s^{−1}. The vast majority of MSPs, however, have velocities less than ~ 130 km s^{−1}

and average just 85 ± 13 km s^{−1}. Assuming this velocity distribution is isotropic, the rms total space velocity of MSPs is expected to be $\langle V^2 \rangle^{1/2} = (\frac{3}{2} V_t^2)^{1/2} = 129$ km s^{−1} with an rms velocity in any one direction of $\langle V_1^2 \rangle^{1/2} = (\frac{1}{2} V_t^2)^{1/2} = 74$ km s^{−1}. Even after excluding proper motion measurements with values less than 4σ , MSPs remain on average a factor of four slower. We present stronger evidence for the suggestion that isolated MSPs have lower velocities than binary MSPs (Johnston, Nicastro, & Koribalski 1998). We note that isolated MSPs are on average two-thirds slower than binary MSPs and so any model for the formation and evolution of isolated MSPs should take this into account.

The implications of such a comparison are, however, mitigated by observational selection effects. Dispersion measure smearing and scattering by the ISM of short-period pulsar signals reduces their detectability. As a consequence the volume surveyed in a blind search for pulsars will be considerably less for MSPs than for slower pulsars. Most of the observed MSPs are isotropically distributed within ~ 1 kpc of the Sun. Because the observed population of MSPs is so ‘local’ it is likely that high velocity pulsars moving perpendicular to the plane of the Galaxy will have been selected against in pulsar surveys. Approximately two thirds of MSPs are found in binaries whereas only ~ 1 per cent of pulsars with periods greater than 100 ms are in binary systems. The space velocity of binary MSPs is expected to increase with decreasing orbital period (Tauris & Bailes 1996). However, searches are less sensitive to short orbital period pulsars because of orbital acceleration effects. Our data do not show any significant correlation between velocity and orbital period. A comprehensive analysis of the observational selection effects is beyond the scope of this paper, however, the 23 MSP velocity measurements are qualitatively consistent with the predictions of the aforementioned MSP models.

Table 1. – continued (Isolated MSPs)

Pulsar	PSR J0711–6830	PSR J1024–0719	PSR J1730–2304	PSR J1744–1134	PSR J2124–3358
R. A. (J2000)	07 ^h 11 ^m 54 ^s .21813(6)	10 ^h 24 ^m 38 ^s .7040(1)	17 ^h 30 ^m 21 ^s .6483(4)	17 ^h 44 ^m 29 ^s .390605(6)	21 ^h 24 ^m 43 ^s .86194(6)
Decl. (J2000)	–68°30′47″.5793(4)	–07°19′18″.849(3)	–23°04′31″.4(1)	–11°34′54″.5716(7)	–33°58′44″.257(1)
PM in R. A. (mas y ^{–1})	–15.7(5)	–41(2)	20.5(4)	18.64(8)	–14(1)
PM in Decl. (mas y ^{–1})	15.3(6)	–70(3)		–10.3(5)	–47(1)
Galactic longitude	279°53	251°70	3°14	14°79	10°93
Galactic latitude	–23°28	40°52	6°02	9°18	–45°44
Period (ms)	5.4909684158061(1)	5.1622045530114(7)	8.1227979128499(2)	4.07454587504741(2)	4.9311148591481(1)
Period derivative (×10 ^{–20})	1.4900(1)	1.873(5)	2.021(1)	0.8940(1)	2.054(1)
Epoch (MJD)	50425.0	50456.0	50320.0	50331.0	50288.0
Dispersion Measure (cm ^{–3} pc)	18.4106(3)	6.495(6)	9.611(2)	3.13775(4)	4.6152(2)
Timing data span (MJD)	49922–50929	49982–50930	49708–50931	49730–50932	49644–50933
RMS timing residual (μs)	2.1	4.6	2.0	0.67	5.2
Number of timing points	108	28	74	94	126

4.1.2 Pulsar dynamics and motion away from the plane

In a study of the proper motions of 26 ordinary pulsars Lyne, Anderson & Salter (1982) demonstrated that pulsars were in general moving away from the Galactic plane; an observation consistent with the view that pulsars are born in a population with a scale height of 70 pc and move away from the plane with a z-velocity of ~ 100 km s^{–1} (Gunn & Ostriker 1970). The work of Harrison, Lyne & Anderson (1993) brought the number of pulsars for which the transverse velocity was not simply an upper limit to 66 and added further weight to this argument. Harrison et al. also showed that the small number of pulsars moving toward the plane must have been born at large z-heights since they were not old enough to have undergone at least a quarter of a period of Galactic oscillation from a birthplace near $z=0$. The lower panel of Fig. 2 shows the motion of the 89 ordinary pulsars with measured proper motions (Taylor, Manchester, & Lyne 1993) over a period of 1 Myr. Although these plots do not take into account the effects of the unknown radial velocity, it is evident that the general motion of ordinary pulsars is directed away from the plane.

For a more accurate measure of the bulk motion of pulsars we chose to eliminate pulsars with velocities less than 4σ . To avoid including pulsars that were still within the progenitor layer ($|z| < 200$ pc) we have also eliminated pulsars with $(\tau_c \times v_z) < 200$ pc, where τ_c is the characteristic age in Myrs and v_z is the component of velocity perpendicular to the plane in km s^{–1}. These criteria leave us with a total of 24 pulsars. The distribution of their Galactic latitude velocity component is symmetric about a mean of 24 ± 55 km s^{–1}. Multiplying these velocities by $b/|b|$ assigns them a positive value if their motion is away from the plane and negative otherwise. The distribution of velocities multiplied by this factor has a similar dispersion but about a mean of 165 ± 43 km s^{–1}. This implies that the majority (20) are moving away from the plane.

The period of oscillation in the Galactic potential for a pulsar on the plane imparted with an initial z-velocity of 100 km s^{–1} is ~ 150 Myrs (Oort 1965). Although large compared with the average age of ordinary pulsars, this time is only a fraction of the typical lifetimes of MSPs (~ 1 Gyr). We

would, therefore, expect MSPs to form a dynamically old population that has reached dynamic equilibrium. Selection effects notwithstanding, we should observe as many MSPs moving toward the plane as away. The upper panel of Fig. 2 illustrates well the apparent isotropy of MSP motion over a period of 3 Myrs. Taking the 17 MSPs with velocities greater than 4σ we find their velocity distribution in b has a mean of -27 ± 16 km s^{–1}. Multiplying these velocities by $b/|b|$ results in a similar mean velocity of -20 ± 17 km s^{–1} suggesting that almost half the pulsars were moving away from the plane. This is in general agreement with the velocity isotropy expected for such an old population.

Another clue to the age of MSPs is evident in their asymmetric drift. A virialised population with a significant radial velocity dispersion will rotate slower about the Galaxy than the local circular speed (Mihalas & Binney 1981). Only an old population is expected to have come close enough to a virialised state to show this effect. The signature of asymmetric drift in this case would be an excess of MSPs moving in the opposite direction to the local flow. To see if this effect was apparent we corrected our proper motion derived velocities for the motion of the Sun with respect to the local standard of rest. Because of the unknown contribution of the radial velocity we removed from our sample those MSPs which had l within 25° of $l=90^\circ$ or 270° , and b within 25° of the Galactic poles. We restricted ourselves to MSPs velocity measurements more significant than 4σ since large errors can reverse the apparent direction of the velocity. This selection leaves us with a total of ten MSPs of which seven are moving in the direction expected of asymmetric drift. The average velocity of these MSPs is 25 ± 12 km s^{–1} directed opposite to the local flow, a clear manifestation of asymmetric drift and of the dynamic equilibrium of the MSP population.

4.1.3 Comparison with scintillation velocities

Of the 13 MSPs for which Johnston et al. (1998) have measured scintillation speeds we have improved arrival-time proper motions for four and new proper motions for six. The scintillation speeds, V_{ISS} , they present were derived using the following equation (Gupta 1995):

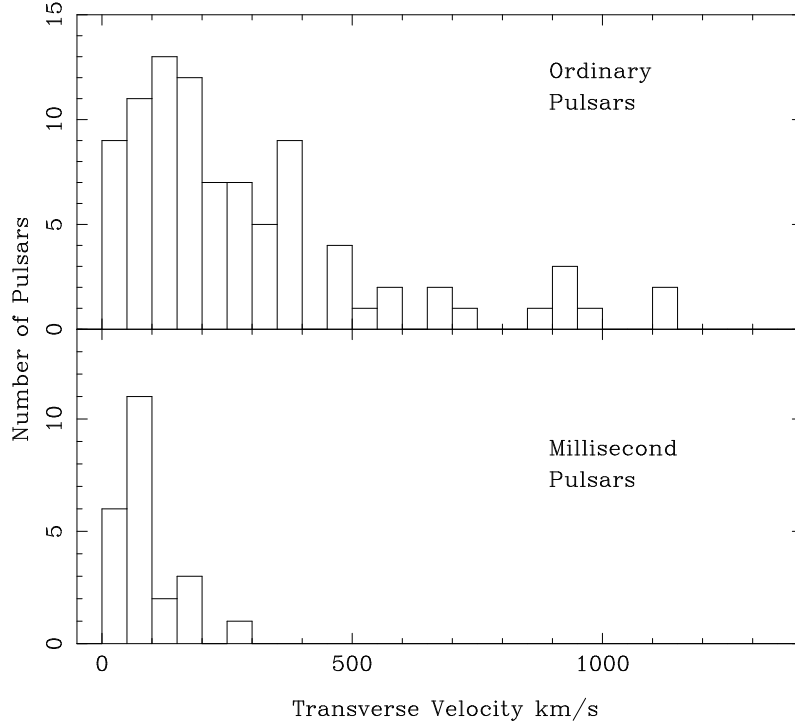


Figure 1. Histograms of transverse velocities for 89 ordinary pulsars ($P > 20$ ms) and 23 millisecond pulsars. The mean transverse velocity for MSPs is 85 ± 13 km s $^{-1}$, approximately a factor of four slower than the mean transverse velocity of ordinary pulsars. A Kolmogorov–Smirnov test shows that the probability that these velocities were drawn from the same distribution is $< 10^{-5}$.

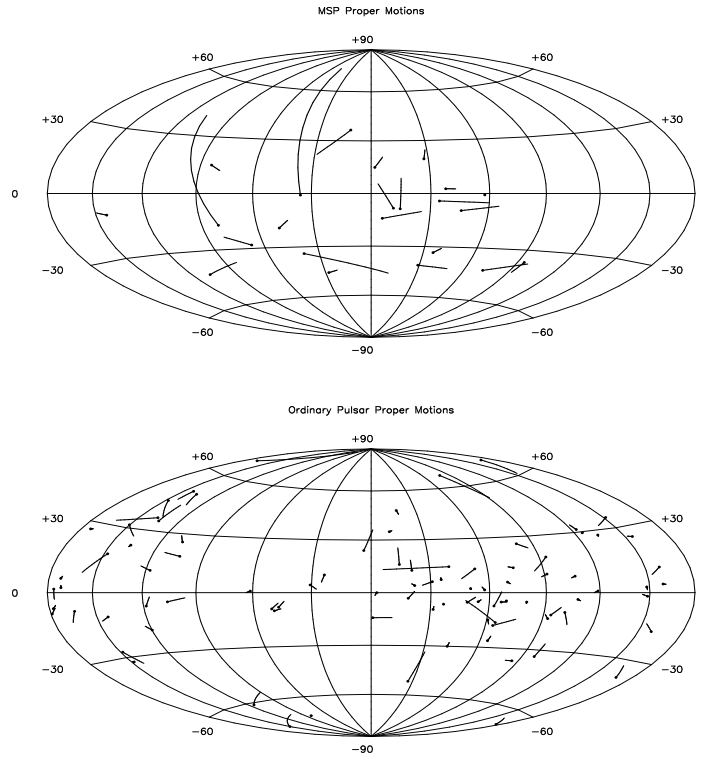


Figure 2. Aitoff–Hammer projections depicting the motion of ordinary and millisecond pulsars. Tracks represent the predicted motion of pulsars over 3 and 1 Myrs for MSPs and ordinary pulsars respectively (the final positions being marked by solid circles). The upper panel shows that almost as many MSPs are moving toward the Galactic plane as away; in contrast to the motion of ordinary pulsars (lower panel) which is in general directed away from the plane.

$$V_{\text{ISS}} = 3.85 \times 10^4 \frac{(D_{\text{kpc}} \Delta\nu_{\text{MHz}} X)^{1/2}}{f_{\text{GHz}} t_{\text{iss},s}} \text{km s}^{-1}. \quad (1)$$

Here D is the distance to the pulsar, f is the observing frequency, t_{iss} and $\Delta\nu$ are respectively the decorrelation time and bandwidth, X is the ratio of observer-screen distance to screen-pulsar distance, and the constant 3.85×10^4 is derived by assuming a Kolmogorov turbulence spectrum for the interstellar medium (Gupta, Rickett, & Lyne 1994).

Johnston et al. found that for 9 MSPs, under the assumption that the screen was located midway between the observer and the pulsar (i.e. $X=1$), the average ratio of the proper motion velocity to the scintillation speed was 1.05. Using our new and improved proper motion velocities we found that for 12 MSPs the average ratio was 0.98. Only for 5 MSPs does the ratio differ from unity by more than 20 per cent: 0.7 for PSR J0437–4715, 0.8 for PSR J2129–5718, 0.6 for PSR J2317+1439, 1.3 for PSR J0711–6830 and 1.4 for PSR J2124–3358. This would suggest that the location of the scattering screen is respectively 30, 36, 29, 64 and 67 per cent of the way to the pulsar. We have not included PSR J2051–0827 for which the scintillation speed is more than a factor of three larger than the proper motion velocity. It is likely that the wind from this MSP's companion is effecting it's scintillation properties (Stappers et al. 1996) and thereby contributing to the discrepancy in velocities.

4.2 The intrinsic spin-down rates of MSPs

4.2.1 Background

The observed spin-down rates for MSPs are approximately six orders of magnitude lower than those of ordinary pulsars. As a consequence the contribution to the measured period derivative, \dot{P}_m , from acceleration effects, cannot be ignored. Damour & Taylor (1991) cite three Doppler accelerations that may bias \dot{P}_m , namely; the effect of Galactic differential rotation (GDR), vertical acceleration in the Galactic potential, and the transverse velocity of the pulsar. We may express the intrinsic spin-down rate as $\dot{P}_i = \dot{P}_m - \delta\dot{P}$ where

$$\delta\dot{P} = P \left[\frac{-v_0^2}{cR_0} \left(\cos l + \frac{(d/R_0) - \cos l}{\sin^2 l + [(d/R_0) - \cos l]^2} \right) \cos b + \frac{v_t^2}{cd} + \frac{a_z}{c} \sin b \right]. \quad (2)$$

The first term in this expression accounts for the effects of GDR with the Sun's galactocentric radius and rotation velocity set to $R_0 = 8.0$ kpc and $v_0 = 220$ km s⁻¹ respectively (Reid 1993). Here l and b are respectively the pulsar's Galactic longitude and latitude. The second term in this equation was first identified by Shklovskii (1970) as the apparent acceleration caused by the transverse velocity of the pulsar v_t at a distance d , while the last term corresponds to the vertical acceleration experienced by the pulsar in the Galactic potential. The magnitude of a_z is derived from the Galactic potential model of Kuijken & Gilmore (1989) and is given by

$$\frac{a_z}{c} = 1.08 \times 10^{-19} \text{s}^{-1} \left[\frac{1.25z}{(z^2 + 0.0324)^{1/2}} + 0.58z \right], \quad (3)$$

where $z = d \sin b$ is the height above the Galactic disc in kpc.

In column 6 of Table 2 we list the derived $\delta\dot{P}$ for the 23 MSPs with known proper motions. The transverse velocities used were derived from the proper motion measurements in column 2. For these MSPs the vertical acceleration term contributes the least to $\delta\dot{P}$ with an average value of $\sim 3 \times 10^{-22}$, while the GDR effect had an average magnitude of $\sim 5 \times 10^{-22}$. By far the most significant effect comes from the transverse velocity term which was on average $\sim 9 \times 10^{-21}$. Column 7 lists the intrinsic period derivatives, \dot{P}_i . In the majority of cases these are significantly less than the measured spin-down rates in column 5.

It is interesting to note that if PSR J1024–0719 is assumed to be at its dispersion measure derived distance of 354 pc then the magnitude of $\delta\dot{P}$ would be larger than that of its measured period derivative. Since the $\delta\dot{P}$ correction of 2.9×10^{-20} is dominated by the transverse velocity term and the proper motion measure is significant, we are certain that the dispersion measure distance is an overestimate. Under the assumption that the measured period derivative is completely due to the transverse velocity we can place a firm, model independent upper limit on the distance to PSR J1024–0719 of 226 pc. A distance to PSR J1024–0719 of 200 pc, consistent with a parallax of $\pi = 5 \pm 4$ mas (at the 1σ level), and consistent with the aforementioned upper limit, was used in our calculations.

4.2.2 Magnetic fields, characteristic ages and death lines for MSPs

Using a magnetic dipole spin-down model with a braking index n , the age of a pulsar, t , may be related to its current period, initial period, P_0 , and spin-down rate thus,

$$t = \frac{P}{(n-1)\dot{P}} \left[1 - \left(\frac{P_0}{P} \right)^{n-1} \right]. \quad (4)$$

Assuming $P_0 \ll P$ and $n=3$ we obtain an expression for the pulsar's 'characteristic age' $t = \tau_c \approx P/(2\dot{P})$. If the surface magnetic field is taken to be dipolar then its magnitude is given by $B \approx 3.2 \times 10^{19} (P\dot{P})^{1/2} \text{G}$, where P is in seconds. The last two columns of Table 2 list B_i and $\tau_{c,i}$, respectively the magnetic field strength and characteristic ages calculated using the intrinsic spin-down rates.

In Fig. 3 we plot magnetic field versus rotation period for the MSPs, showing the magnitude of the correction to the measured spin-down rate. The correction applied not only results in a decrease in the derived magnetic field strength but also an increase in characteristic age. Fig. 3 shows that, of the 23 MSPs, ten are found to have ages close to or greater than 10 Gyr (the so-called 'Hubble limit'). The apparent paradox of MSPs with ages greater than that of the Galaxy (9 ± 2 Gyr; Winget et al. 1987) may be resolved in several ways (Camilo, Thorsett, & Kulkarni 1994). Firstly, the assumption that $P_0 \ll P$ may be incorrect, and in fact, the 'oldest' MSPs are born with initial periods close to their current values. This would suggest that the mass accretion rate in low-mass systems is well below the Eddington-limited rate. Secondly, the braking index may be greater than three because of multipolar magnetic field structure or angular momentum loss to gravitational radiation or indeed is time variable. If MSPs do, however, possess true ages comparable to the age of the Galaxy then their study would offer us

Table 2. Derived quantities for MSPs with measured proper motions

Pulsar	μ (mas y ⁻¹)	Distance (kpc)	Velocity (km s ⁻¹)	\dot{P}_m (10 ⁻²⁰)	$\delta\dot{P}$ (10 ⁻²⁰)	\dot{P}_i (10 ⁻²⁰)	B_i (10 ⁸ G)	$\tau_{c,i}$ (Gy)
J0437–4715	140.7(3)	0.180	120.5(2)	5.730	4.932	0.7975	3.0	6.0
J0613–0200	7(1)	2.190	77(11)	0.9570	0.1207	0.836	1.6	5.8
J0711–6830	22.0(6)	1.039	78(2)	1.490	0.6557	0.8341	2.2	10
J1024–0719	81(4)	0.200	62(3)	1.873	1.574	0.2989	1.3	27
J1045–4509	7(2)	3.246	52(15)	1.767	0.1312	1.636	3.5	7.2
B1257+12	95.0(8)	0.624	284(2)	11.43	8.612	2.821	4.2	3.5
J1455–3330	24(13)	0.738	100(54)	2.423	0.9043	1.519	3.5	8.3
J1603–7202	8.6(7)	1.636	27(2)	1.571	0.4610	1.110	4.1	21
J1643–1224	8(5)	4.860	159(99)	1.847	0.8721	0.9751	2.2	7.5
J1713+0747	6.4(2)	1.111	28.2(9)	0.8536	0.1025	0.7511	1.9	9.6
J1730–2304	>20.2(4)	0.509	>51(1)	2.021	>0.4664	<1.554	<3.6	>8.3
J1744–1134	21.3(4)	0.370	33.1(6)	0.8941	0.1810	0.7131	1.7	9.1
B1855+09	6.16(7)	1.000	17.3(2)	1.784	0.05056	1.733	3.1	4.9
J1911–1114	24(13)	1.588	183(99)	1.415	0.8383	0.5764	1.5	10
B1937+21	0.48(1)	3.580	79(2)	10.51	–0.0467	10.56	4.1	0.23
B1957+20	30.4(8)	1.533	190(5)	1.685	0.5380	1.147	1.4	2.2
J2019+2425	23(2)	0.912	83(7)	0.7022	0.4529	0.2491	1.0	25
J2051–0827	5(3)	1.300	14(8)	1.272	0.07892	1.193	2.3	6.0
J2124–3358	49(2)	0.247	53(2)	2.054	0.7547	1.300	2.6	6.0
J2129–5721	8(4)	2.550	56(28)	2.068	0.2569	1.811	2.6	3.3
J2145–0750	18(2)	0.500	38(4)	2.986	0.7794	2.207	6.0	12
J2317+1439	7(4)	1.892	94(53)	0.2423	0.09165	0.1504	0.73	36
J2322+2057	24(4)	0.782	80(13)	0.9741	0.5504	0.4236	1.4	18

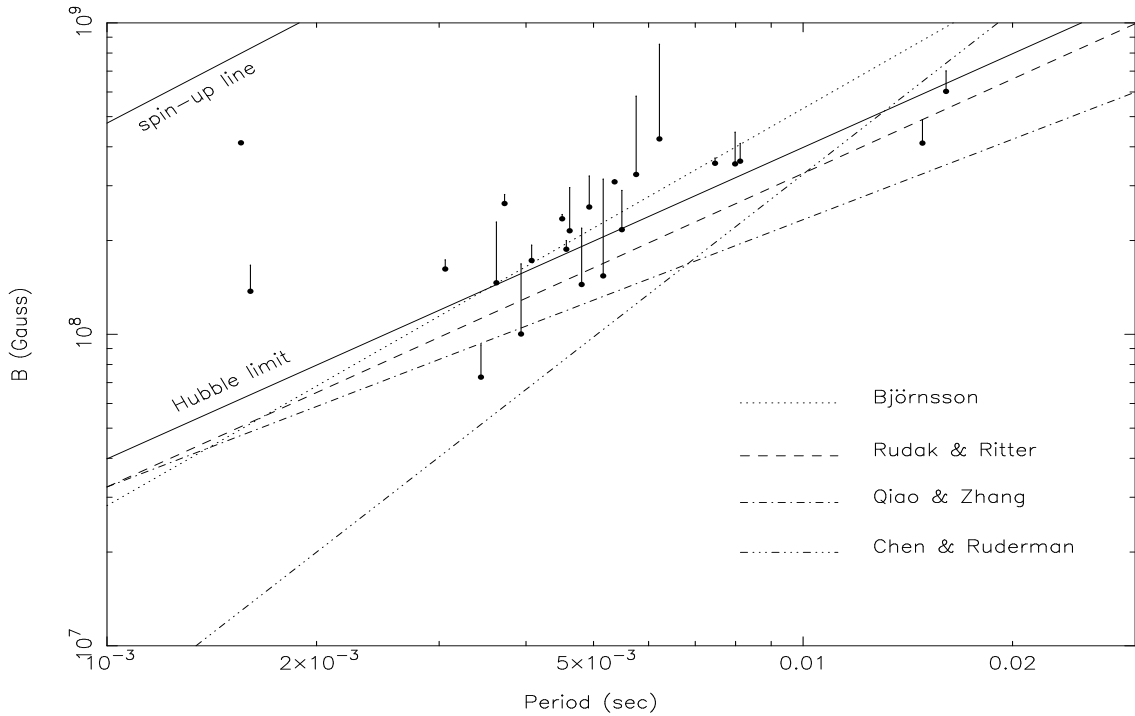


Figure 3. Magnetic field–Period diagram for the 23 MSPs with measured velocities. Tracks show the change in position of MSPs in the B – P plane when corrections are made to the spin-down rate to compensate for apparent Doppler accelerations. The positions corresponding to the intrinsic spin-down rates are marked by solid circles. Also plotted are several death lines for MSPs, the Hubble limit (corresponding to an age of 10^{10} years), and the spin-up line (see text).

the exciting prospect of investigating the earliest processes of star formation in our Galaxy.

Most models of the spin-down evolution of pulsars predict a cessation of radio emission when electron-positron pairs can no longer be produced. The region of the B - P space where the emission terminates for a particular pulsar depends upon the structure and magnitude of its magnetic field and defines the so-called ‘death valley’ for long-period pulsars (Chen & Ruderman 1993). The attempts to define an equivalent ‘death line’ for short-period pulsars (Rudak & Ritter 1994; Qiao & Zhang 1996; Björnsson 1996) have been plotted in Fig. 3. We note that no single death line falls below all the points.

5 CONCLUSIONS

In this paper we have presented improved timing parameters for 13 MSPs including nine new proper motion measurements. Combining these results with previous measurements brings the number of measured MSP velocities to 23. The analysis of these velocities have lead to the following conclusions:

- The transverse velocity distribution of MSPs has a mean value of $85 \pm 13 \text{ km s}^{-1}$; approximately a factor of four slower than the mean transverse velocity of ordinary pulsars. The MSP velocity distribution we derived is qualitatively consistent with the models of Tauris & Bailes (1996) and Cordes & Chernoff (1997), and the scintillation speeds measured by Johnston et al. (1998).
- MSPs form a dynamically old population. As expected for a population that has reached dynamic equilibrium, almost as many MSPs are moving toward the Galactic plane as away. This is in contrast with the young population of ordinary pulsars which have a bulk motion directed away from the plane. MSPs also show an asymmetric drift characteristic of a virialised population.
- Our corrections to the spin-down rate of MSPs result in increases in characteristic ages and decreases in the derived surface magnetic field strengths. In particular, almost half of the MSPs for which this correction has been made have characteristic ages comparable to, or greater than, the age of the Galaxy. Such large ages may be accounted for if the birth periods are close to the current periods.

REFERENCES

- Alpar M. A., Cheng A. F., Ruderman M. A., Shaham J., 1982, *Nat*, 300, 728
- Arzoumanian Z., Fruchter A. S., Taylor J. H., 1994, *ApJ*, 426, L85
- Backer D. C., Kulkarni S. R., Heiles C., Davis M. M., Goss W. M., 1982, *Nat*, 300, 615
- Bailes M. et al., 1994, *ApJ*, 425, L41
- Bailes M. et al., 1997, *ApJ*, 481, 386
- Bailes M., Manchester R. N., Kesteven M. J., Norris R. P., Reynolds J. E., 1990, *MNRAS*, 247, 322
- Bell J. F., Bailes M., Manchester R. N., Weisberg J. M., Lyne A. G., 1995, *ApJ*, 440, L81
- Bhattacharya D., van den Heuvel E. P. J., 1991, *Phys. Rep.*, 203, 1
- Bignami G. F., Caraveo P. A., 1988, *ApJ*, 325, L5
- Björnsson C.-I., 1996, *ApJ*, 471, 321
- Blaauw A., 1961, *Bull. Astron. Inst. Netherlands*, 15, 265
- Blandford R., Teukolsky S. A., 1976, *ApJ*, 205, 580
- Camilo F., Foster R. S., Wolszczan A., 1994, *ApJ*, 437, L39
- Camilo F., Nice D. J., Taylor J. H., 1996, *ApJ*, 461, 812
- Camilo F., Thorsett S. E., Kulkarni S. R., 1994, *ApJ*, 421, L15
- Chanmugam G., Brecher K., 1987, *Nat*, 329, 696
- Chen K., Ruderman M., 1993, *ApJ*, 408, 179
- Cordes J. M., 1986, *ApJ*, 311, 183
- Cordes J. M., Chernoff D. F., 1997, *ApJ*, 482, 971
- Damour T., Taylor J. H., 1991, *ApJ*, 366, 501
- Fomalont E. B., Goss W. M., Lyne A. G., Manchester R. N., Justtanont K., 1992, *MNRAS*, 258, 497
- Fomalont E. B., Goss W. M., Manchester R. N., Lyne A. G., 1997, *MNRAS*, 286, 81
- Gott J. R., Gunn J. E., Ostriker J. P., 1970, *ApJ*, 160, L91
- Gunn J. E., Ostriker J. P., 1970, *ApJ*, 160, 979
- Gupta Y., 1995, *ApJ*, 451, 717
- Gupta Y., Rickett B. J., Lyne A. G., 1994, *MNRAS*, 269, 1035
- Hansen B. M. S., Phinney E. S., 1997, *MNRAS*, 291, 569
- Harrison P. A., Lyne A. G., Anderson B., 1993, *MNRAS*, 261, 113
- Helfand D. J., Taylor J. H., Manchester R. N., 1977, *ApJ*, 213, L1
- Johnston S., Nicastro L., Koribalski B., 1998, *MNRAS*, 297, 108
- Kaspi V. M., Taylor J. H., Ryba M., 1994, *ApJ*, 428, 713
- Kuijken K., Gilmore G., 1989, *MNRAS*, 239, 571
- Lorimer D. R., Lyne A. G., Bailes M., Manchester R. N., D’Amico N., Stappers B. W., Johnston S., Camilo F., 1996, *MNRAS*, 283, 1383
- Lorimer D. R. et al., 1995, *ApJ*, 439, 933
- Lyne A. G., Anderson B., Salter M. J., 1982, *MNRAS*, 201, 503
- Lyne A. G., Lorimer D. R., 1994, *Nat*, 369, 127
- Lyne A. G., Manchester R. N., Lorimer D. R., Bailes M., D’Amico N., Tauris T. M., Johnston S., 1998, *MNRAS*, 295, 743
- Manchester R. N. et al., 1996, *MNRAS*, 279, 1235
- Manchester R. N., Taylor J. H., Van Y.-Y., 1974, *ApJ*, 189, L119
- Mihalas D., Binney J., 1981, *Galactic Astronomy*, (New York: W. H. Freeman)
- Navarro J., 1994, PhD thesis, California Institute of Technology
- Nice D. J., Taylor J. H., 1995, *ApJ*, 441, 429
- Oort J. H., 1965, *Stars and Stellar Systems*, V, 455
- Qiao G. J., Zhang B., 1996, *A&A*, 306, L5
- Radhakrishnan V., Srinivasan G., 1981, in *Proc. 2nd Asian-Pacific Regional Meeting of the IAU*, ed. B. Hidayat & M. W. Feast, (Jakarta: Tira Pustaka), p. 423
- Rawley L. A., Taylor J. H., Davis M. M., 1988, *ApJ*, 326, 947
- Reid M. J., 1993, *ARA&A*, 31, 345
- Rudak B., Ritter H., 1994, *MNRAS*, 267, 513
- Sandhu J. S., 1999, PhD thesis, California Institute of Technology

- Sandhu J. S., Bailes M., Manchester R. N., Navarro J., Kulkarni S. R., Anderson S. B., 1997, *ApJ*, 478, L95
- Shklovskii I. S., 1970, *SvA*, 13, 562
- Standish E. M., 1982, *A&A*, 114, 297
- Stappers B. W. et al., 1996, *ApJ*, 465, L119
- Stappers B. W., Bailes M., Manchester R. N., Sandhu J. S., Toscano M., 1998, *ApJ*, 499, L183
- Tauris T. M., Bailes M., 1996, *A&A*, 315, 432
- Taylor J. H., Manchester R. N., Lyne A. G., 1993, *ApJS*, 88, 529
- Taylor J. H., Weisberg J. M., 1989, *ApJ*, 345, 434
- Trimble V., 1971, in *The Crab Nebula: IAU Symposium 46*, ed. R. D. Davies & F. G. Smith, (Reidel: Dordrecht), p. 12
- Winget D. E., Hansen C. J., Liebert J., Van Horn H. M., Fontaine G., Nather R. E., Kepler S. O., Lamb D. Q., 1987, *ApJ*, 315, L77
- Wolszczan A., 1994, *Sci*, 264, 538
- Wyckoff S., Murray C. A., 1977, *MNRAS*, 180, 717